Effect of cohesion on local compaction and granulation of sheared granular materials

Sudeshna Roy[1,⋆], *Stefan* Luding[1,⋆⋆], and *Thomas* Weinhart[1,⋆⋆⋆]

[1] *Multi Scale Mechanics (MSM), MESA+, CTW, University of Twente, PO Box 217, 7500 AE Enschede, The Netherlands*

Abstract. This paper results from an ongoing investigation of the effect of cohesion on the compaction of sheared wet granular materials. We compare the spatial distribution of the volume fraction of dry non-cohesive and moderately-to-strongly wet cohesive granular materials. Here we report the effect of cohesion between the grains on bulk compaction, i.e. the volume fraction, in a three dimensional system. We study this in an unconfined, slowly sheared split-bottom ring shear cell, where materials while sheared are subjected to compression under the confining weight of the materials above. Our results show that the inter-particle cohesion has a considerable impact on the bulk compaction of the materials. For weak cohesion we observe dilation while strong cohesion leads to granulation already for Bond numbers $Bo \gtrsim 1.0$.

1 Introduction

Unsaturated granular media of particles with interstitial liquid in the form of bridges between particle pairs, display bulk cohesion, which can be tuned using different liquids with varying surface tension σ. Earlier experimental studies have been done on the slow shear and compaction dynamics of wet granular assemblies subjected to tapping [1]. The influence of the liquid surface tension σ on the compaction dynamics has shown a decrease of both initial and final packing fractions as a function of σ [2]. This behavior is limited to weak and moderately cohesive systems.

Fournier et al. [3] did not observe a measurable dependence of packing densities on the amount of wetting liquid added, an obvious reason being that the forces exerted by the bridges are only very weakly dependent on bridge volume [4]. At small liquid content and after sufficient equilibration, the interior of the wet granulate is expected to be characterized by a network of liquid bridges connecting adjacent grains. It is clear that the connectivity of this network of liquid bridges is of importance for the mechanics of the wet granular materials [5–7], be it directly due to the capillary forces itself or due to the enhancement of the mutual friction between the grains by the increased internal pressure. For the wet granular materials, this pressure increase is of the order $\Delta p \approx \sigma/r$ given by the Laplace-Young equation, where r is a typical radius of the grains. The local volume fraction of the bulk on macro-scale is connected to the pressure gradient and is thus dependent on σ/r.

⋆ e-mail: s.roy@utwente.nl
⋆⋆ e-mail: s.luding@utwente.nl
⋆⋆⋆ e-mail: t.weinhart@utwente.nl

We study here the packing fraction in the critical state for non-cohesive to strongly cohesive systems by varying the surface tension of the liquid. Wet granular are cohesive and particles can stick together and form local agglomerates or granules, due to formation of clusters of particles for very cohesive systems, as shown in figure 1 and 4(c).

2 Model System

2.1 Geometry

Split-Bottom Ring Shear Cell: We use MercuryDPM [8, 9], an open-source implementation of the Discrete Particle Method, to simulate a shear cell with annular geometry and a split bottom plate, as explained in [10]. Earlier studies used similar rotating set-ups, including [11–13]. The geometry of the system consists of an outer cylinder (radius $R_o = 110$ mm) rotating around a fixed inner cylinder (radius $R_i = 14.7$ mm) with a rotation frequency of $\Omega = 2\pi f$ and $f = 0.01$ revolutions per second (see Figure 1). The granular material is confined by gravity between the two concentric cylinders and the bottom plate, with a free top surface. The bottom plate is split at radius $R_s = 85$ mm. Due to the split at the bottom, a narrow shear band is formed. It moves inwards and widens towards the flow surface. This set-up thus features a wide shear band away from the bottom and the wall which is free from boundary effects. The shear cell is filled with particles of mean diameter $d_p \approx 2.2$ mm up to filling height of $H \approx 40$ mm under dry conditions. Thus, the shear band remains far away from the inner wall.

In earlier studies [14–16], a quarter of this system ($0° \leq \phi \leq 90°$) was simulated using periodic boundary conditions. In order to save computation time, here we simulate

only a smaller section of the system ($0° \leq \phi \leq 30°$) with appropriate periodic boundary conditions in the angular coordinate, unless specified otherwise. We have observed no noticeable effect on the macroscopic behavior in comparisons between simulations done with a smaller (30°) or larger (90°) opening angle. Note that for very strong attractive forces, the system becomes inhomogeneous and looses its radial symmetry: i.e. agglomeration of particles occurs. Then, particles interact on a larger length scale and thus the above statement is not true anymore.

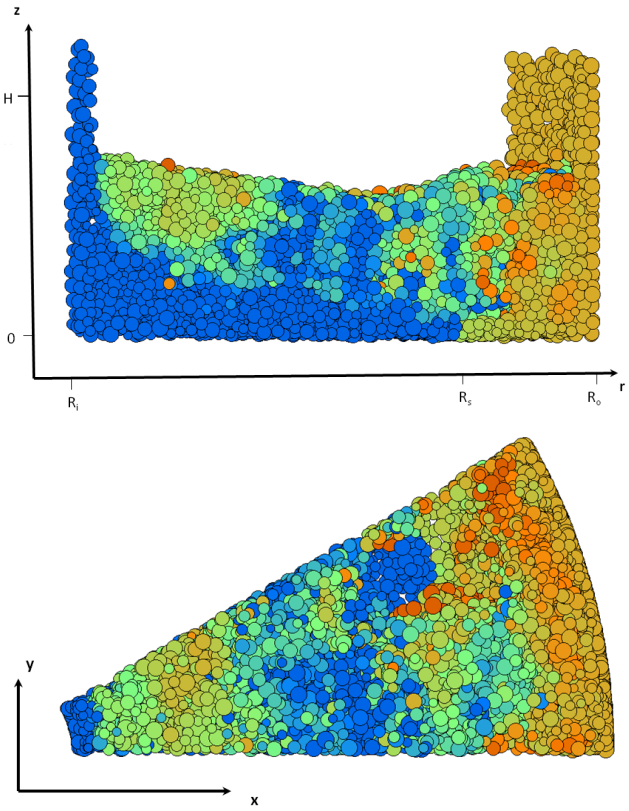

Figure 1: a) Front view and b) Top view of highly cohesive wet granular materials ($Bo_g = 34.6$). Different colors blue, green and red denote the measure of low to high kinetic energy of the particles.

2.2 Contact model and parameters

We use a linear visco-elastic slightly frictional contact model in combination with Willet's capillary bridge model, as explained in [10]. In order to see the effect of varying cohesive strength on the macroscopic rheology of wet materials, we vary the intensity of the maximum capillary force ${f_c}^{\max} = \pi d\sigma \cos\theta$, by varying the surface tension of the liquid σ, while keeping the volume of liquid bridges constant, ($V_\mathrm{b} = 75$ nl), corresponding to a liquid saturation of 8% of the volume of the pores. We compare here the volume fractions of non-cohesive to moderate to strongly cohesive granular materials, with surface tension of liquid ranging from $\sigma = 0$ Nm^{-1},up to $\sigma = 5$ Nm^{-1} for strongly cohesive systems. The contact angle is fixed at $\theta = 10°$.

3 Dimensionless numbers

The effects of varying shear rate, pressure, stiffness and cohesion can be modelled using three dimensionless numbers, expressed as a ratio of time-scales as given in Tab. 1, where the subscripts $\dot{\gamma}, p, k$ and c denote strain-rate, pressure, stiffness and cohesion respectively [17].

Table 1: Dimensionless numbers for the model

Dimensionless number	Definition	Time scale ratio
Inertial number I	$\frac{\dot{\gamma} d_p}{\sqrt{p/\rho}}$	$t_p/t_{\dot{\gamma}}$
Softness p^*	$\frac{p d_p}{k_{\max}}$	$(t_k/t_p)^2$
Local Bond number Bo	$\frac{{f_c}^{\max}}{p {d_p}^2}$	$(t_p/t_c)^2$

In addition, we define the *global* Bond number as $Bo_g = {f_c}^{\max}/(p_{\mathrm{mean}} {d_p}^2)$, where p_{mean} is the mean pressure in the system (at about half filling height $H/2$).

4 Rheological model

The macroscopic quantities are obtained by spatial coarse graining with temporal averaging of the system in steady state as detailed in [10, 17]. We study the effect of the local Bond number Bo on the local volume fraction ϕ in the critical state. This state is reached only after large enough shear, when the materials deform with applied strain without detectable changes in the local quantities, independent of the initial condition. This corresponds to the region of the shear band center in the system, as explained in detail in [17].

4.1 Non-cohesive granular materials

For dry granular materials, $Bo = 0$, the rheology only depends on p^* and I. The dependence of the macroscopic friction coefficient $\mu = \tau/p$ on p^* and I has been studied in [15–17]. In order to complete the rheology for soft, compressible particles, a relation for the solid volume fraction (packing fraction) as function of pressure and shear rate is missing for dry non-cohesive materials. In [18], the following dependency was observed:

$$\phi(I, p^*) = \phi_o f_I(I) f_p(p^*) \tag{1}$$

with the critical or steady state density under shear, in the limit of vanishing pressure and inertial number, $\phi_o = 0.64$, $f_p(p^*) = (1 + p^*/{p_o}^*)$, $f_I(I) = (1 - I/I_o)$. The typical strain rate for which dilation would turn to fluidization is $I_o = 0.85$, and the typical pressure level for which softness leads to huge densities is ${p_o}^* = 0.33$ [18]. Note that both correction functions are first order, i.e. they are valid only for sufficiently small arguments. Too large inertial numbers would fully fluidize the system so that the rheology should be that of a granular fluid, for which kinetic theory applies, while too large pressure would lead to enormous overlaps, for which the contact model and the particle simulation become questionable.

4.2 Cohesive granular materials

Additional corrections for cohesive particles involve the so-called Bond-number Bo which is the subject of our study. Agreeing with the convention of a generalised rheology [18], the additional correction $f_c(Bo)$ for cohesion is included:

$$\phi(I, p^*, Bo) = \phi_o f_I(I) f_p(p^*) f_c(Bo) \tag{2}$$

Table 2: Coefficients for the model

Dimensionless number	Corrections	Coefficients
Volume fraction (ϕ_o)		$\phi_o = 0.65$
Inertial number (I)	$f_I = \left(1 - \frac{I}{I_o}\right)$	$I_o = 0.85$
Softness (p^*)	$f_p = \left(1 + \frac{p^*}{{p_o}^*}\right)$	${p_o}^* = 0.27$
Cohesion (Bo)	$f_c = \exp\left(-\frac{\min(Bo,1)}{Bo_{c1}}\right) \times \left(1 + \frac{\max(Bo-1,0)}{Bo_{c2}}\right)$	$Bo_{c1} \approx 215$, $Bo_{c2} \approx 93$ (2D plot) and $Bo_{c1} \approx 218$, $Bo_{c2} \approx 85$ (3D plot)

5 Results: packing fraction and local clustering

We analyse the local packing fraction ϕ as a function of the local Bond number Bo. All the data shown in figure 2 corresponds to the critical state, though a shear band is not clearly defined in strongly cohesive systems ($Bo_g > 3.46$). The packing fraction decreases (weakly) with Bo up to a local critical Bond number $Bo_c = 1.0$, then increases linearly with further increase in Bond number Bo ($Bo > Bo_c$) as shown in figure 2. This indicates that local compaction of granular materials occurs when the maximum attractive capillary force exceeds the repulsive force due to the local confining pressure p i.e. $pd_p{}^2 < f_c{}^{max}$, resulting in some material densification. This result is conceptually in the same spirit as the results of [15]. Singh et al. [15] shows the effect of dry cohesion (local Bond number) on width and position of the shear band and states that both are independent of cohesion for $Bo < 1.0$. However, the band becomes wider and moves inwards for $Bo > 1.0$. Here, we see a similar effect for wet cohesion on the local packing fraction of the materials. The local density of materials increases by 25% from non-cohesive ($Bo_g = 0$) to strongly cohesive granular materials ($Bo_g = 34.6$). Further, the effects of other dimensionless numbers I and p^* are also present for wet cohesive granular materials as they exist for dry granular materials. These effects are combined as individual corrections and they collectively contribute to the local bulk density of the material.

The correction f_c is given by the solid line in figure 2, which is a representation of $\phi/(f_I f_p)$ as a function of the local Bond number Bo. We observe different phenomenological changes in the local density for small and large cohesion, and thus $f_c(Bo)$ is fitted separately by :

$$f_c(Bo) = \begin{cases} f_{c1} = \exp(-Bo/Bo_{c1}) \text{ for } Bo \leq 1.0, \\ f_{c2} = 1 + (Bo - 1)/Bo_{c2} \text{ for } Bo > 1.0 \end{cases} \tag{3}$$

$Bo \leq 1.0$ and $Bo > 1.0$, respectively (see Tab. 2), where f_{c1} is valid for range of Bond number $Bo \leq 1.0$, f_{c2} is valid for Bond number $Bo > 1.0$. As the data accuracy does not allow a good fit of f_{c1}, we propose to improve the function f_{c1} with better data quality in future.

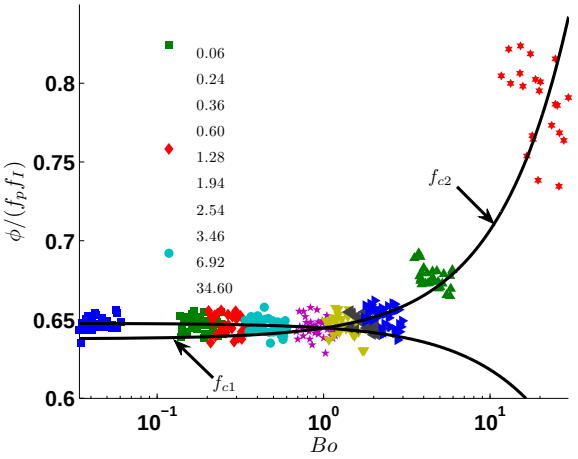

Figure 2: Scaled local packing fraction $\phi/(f_I f_p)$ as a function of the local Bond number Bo. The solid lines are given by Eq. (3), with parameters given in Tab. 2.

To validate the effect of each dimensionless number, contributing in the multiplicative correction forms, as shown in Eq. (2), we represent in a surface plot ϕ/f_I as a function of Bo and p^*, as shown in figure 3. As the flow is quasistatic, the inertial number effect is very weak. The data are fitted by two surfaces, differentiated by $Bo \leq 1$ and $Bo > 1$ respectively, given by equations $f_p f_{c1}$ and $f_p f_{c2}$ respectively with the coefficients given in Tab. 2. The two surfaces are obtained by fitting data for $Bo \leq 1.0$ and $Bo > 1.0$ respectively, eliminating the inhomogeneous data for strong cohesion $Bo_g = 34.6$ in order to get good agreement. The fitting constants for the surface plots are given in Tab. 2. The local volume fraction for dry non-cohesive is approximately equal to ϕ_o and is also in agreement with the trend (not shown in the figure).

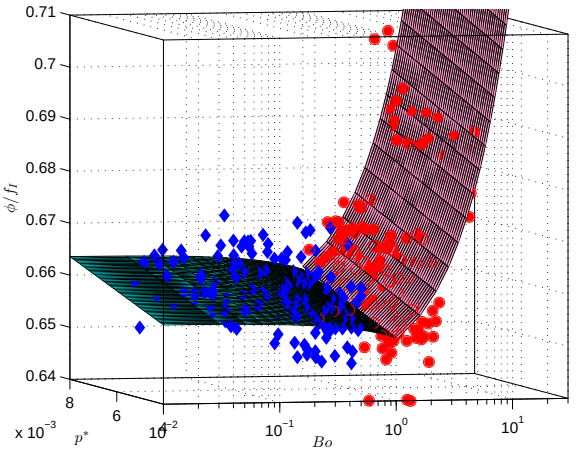

Figure 3: Surface plot of ϕ/f_I as a function of p^* and Bo with $Bo \leq 1.0$ (blue ◆) and $Bo > 1.0$ (red •).

Figure 4 (a), (b) and (c) shows the contour plot of the spatial distribution of local packing fraction with the magnitude given by the color map for different Bond numbers $Bo_g = 0, 1.94$ and 34.6 respectively. Focusing on the center of the shear band, the mean volume fraction is close to 0.65 for non-cohesive materials as shown in figure 4(a). In comparison, the local volume fraction of the strongly cohesive materials inside the center of the shear band is 0.85 in figure 4(c). The vertical center of mass of the materials decreases by 1% from the non-cohesive (a) to the moderate cohesion (b) and by 25% for strong cohesion (c).

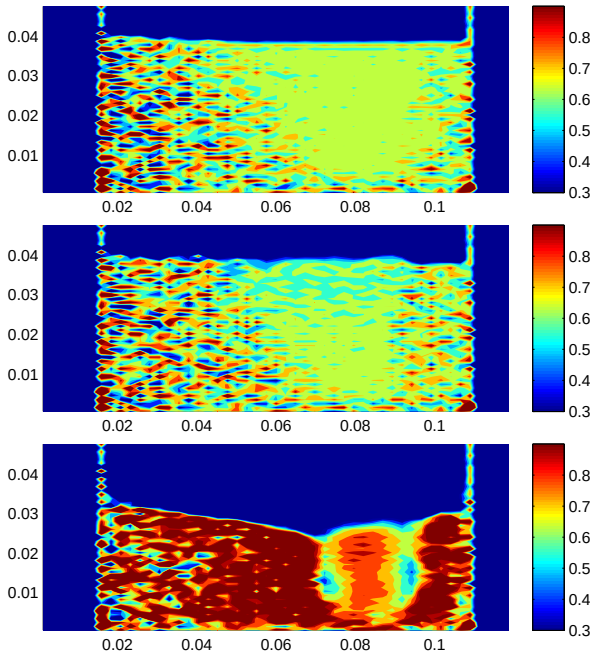

Figure 4: Contour plot of volume fraction for (a) $Bo_g = 0.0$, (b) $Bo_g = 1.94$ and (c) $Bo_g = 34.6$ in the $r - z$ plane. Both (a) and (b) are homogeneous in cylindrical direction, while (c) displays granule formation as shown in figure 1.

6 Conclusion

We studied the local packing fraction of dry and wet granular materials as a function different dimensionless numbers, namely, the inertial number I, the softness p^* and the Bond number Bo. Focus is on the effect of cohesion (quantified by the Bond number). Earlier studies have shown that the packing fraction of dry granular materials is to the first order linearly dependent on I and p^*. We observe the same scalings for wet materials. Further, the packing fraction is slightly decreasing for small Bond numbers ($Bo \leq 1.0$) and linearly increasing for overall high Bond numbers ($Bo > 1.0$). The rheology is defined by a generalised model which constitutes the correction terms in multiplicative form. Our results show that for strongly cohesive systems, materials are densely compacted and the filling height of the bed drops by approximately 25%, which corresponds to an increase in volume fraction by 20% in the range from non-cohesive to strongly cohesive granular materials. The generalised model is validated by our data where the parameters are in close agreement with that of earlier validated coefficients for non-cohesive granular materials. To have a complete understanding of the rheology, focus on a generalised rheology for the coordination number would be interesting.

Acknowledgements

We acknowledge our financial support through Technologiestichting STW Project 12272.

References

[1] J. Fiscina, G. Lumay, F. Ludewig, N. Vandewalle, Physical Review Letters **105**, 048001 (2010)

[2] P. Rognon, J.N. Roux, D. Wolf, M. Naaim, F. Chevoir, Europhys. Lett. **74**, 644 (2006)

[3] Z. Fournier, D. Geromichalos, S. Herminghaus, M.M. Kohonen, F. Mugele, M. Scheel, M. Schulz, B. Schulz, C. Schier, R. Seemann et al., J. Phys.: Condens. Matter **17**, S477 (2005)

[4] C.D. Willett, M.J. Adams, S.A. Johnson, J. Seville, Langmuir **16**, 9396 (2000)

[5] T. Mikami, H. Kamiya, M. Horio, Chem. Eng. Sci. **5** (1998)

[6] D. Geromichalos, M.M. Kohonen, F. Mugele, S. Herminghaus, Physical review letters **90**, 168702 (2003)

[7] S. Simons, Powder Technology **87**, 29 (1996)

[8] A. Thornton, T. Weinhart, S. Luding, O. Bokhove, Int. J. Mod. Phys. C **23, 124001** (2012)

[9] T. Weinhart, A. Thornton, S. Luding, O. Bokhove, Granul. Matter. **14**, 289 (2012)

[10] S. Roy, A. Singh, S. Luding, T. Weinhart, Computational Particle Mechanics **102**, 449–462 (2015)

[11] S. Schöllmann, Phys. Rev. E **59**, 889 (1999)

[12] X. Wang, H.P. Zhu, A.B. Yu, Granular Matter **14**, 411 (2012)

[13] E. Woldhuis, B.P. Tighe, W. Saarloos, The European Physical Journal E: Soft Matter and Biological Physics **28**, 73 (2009)

[14] S. Roy, S. Luding, T. Weinhart, Procedia Engineering **102**, 1531 (2015)

[15] A. Singh, V. Magnanimo, K. Saitoh, S. Luding, Phys. Rev. E **90**, 022202 (2014)

[16] A. Singh, V. Magnanimo, K. Saitoh, S. Luding, New J. Phys. **17**, 043028 (2015)

[17] S. Roy, S. Luding, T. Weinhart, arXiv preprint arXiv:1609.03098 (2016)

[18] S. Luding, A. Singh, S. Roy, D. Vescovi, T. Weinhart, V. Magnanimo, The 7th International Conference on Discrete Element Methods. (2016)